

RARE HADRONIC B DECAYS

J. R. FRY

Department of Physics, University of Liverpool, PO Box 147 Liverpool, L69 7ZE, England
E-mail: J.R.Fry@liverpool.ac.uk

Recent data from the rare decays of B mesons into hadronic final states is presented from BaBar, Belle, CDF and CLEO. Where possible the data are compared with theoretical calculations, with the twin aims of further testing the Standard Model and searching for evidence of new physics. A brief description is given of some theoretical approaches in order to indicate which decays are the most sensitive for further study.

1. Introduction

Updated branching fractions (BF) and CP-asymmetries (A_{CP}) are presented for rare decays of B_d and B_u mesons into hadronic final states. By rare we typically mean processes having BF of less than 10^{-5} . In the main these rare decay modes are charmless and involve final states in which no charmed quarks are produced. The reason for studying rare decay modes is that the Standard Model is a good approximation to reality at current energies: it gives a very good description of the more common processes in particle interactions, including CP-violation in K^0 and B^0 decays. Thus we need to consider processes where the Standard Model amplitudes are small if we are to be sensitive to new physics. This generally implies decays dominated by (second order) penguin diagrams, or CKM-suppressed decays.

Because of the dependence of the values of BF and A_{CP} on angles of the unitarity triangle in cases where more than one amplitude contributes to the decay process, the study of rare decays gives an alternative route to the measurement of the parameters ρ and η and hence additional constraints on the unitarity triangle. Disagreement between the values of the parameters of the unitarity triangle obtained in this way and those obtained through direct measurement of time-dependent asymmetries could provide an indication for new physics. However, given the difficulties in making theoretical calculations, and the approximations and model-dependent assumptions that are often made, it could also indicate that refinements to our understanding of hadron dynamics are needed. In this situation model-independent calculations are of great value in assessing the difference between experimental measurements and expectation from the Standard Model, even if the constraints they impose are somewhat weaker than those

from QCD-based theories.

1.1. Direct CP-Violation

Direct CP-violation is observed when the branching fraction for the decay of a B meson into a particular final state is different from that of its antiparticle into the charge-conjugate final state. It can be measured for both charged and neutral B mesons, although the former is usually easier to do, and gives higher precision, since charged B mesons are self-tagging. It is usual to consider the CP-asymmetry, A_{CP} , which is the difference in branching fractions for charge-conjugate decays divided by the sum, since many acceptance-dependent systematic effects cancel to first order. Direct CP-violation occurs if the decay $B \rightarrow f$ (and its charge-conjugate) is mediated by two amplitudes^a with different strong and weak phases. Writing the decay amplitudes:

$$a_f = a_1 e^{i(\delta_1 + \phi_1)} + a_2 e^{i(\delta_2 + \phi_2)}$$
$$\bar{a}_{\bar{f}} = a_1 e^{i(\delta_1 - \phi_1)} + a_2 e^{i(\delta_2 - \phi_2)}$$

where δ is the (CP-even) strong phase and ϕ the (CP-odd) weak phase, A_{CP} may be written as the difference of the amplitudes-squared divided by the sum:

$$A_{CP} = \frac{|\bar{a}_{\bar{f}}|^2 - |a_f|^2}{|\bar{a}_{\bar{f}}|^2 + |a_f|^2}$$
$$= \frac{2a_1 a_2 \sin(\delta_2 - \delta_1) \sin(\phi_2 - \phi_1)}{a_1^2 + a_2^2 + 2a_1 a_2 \cos(\delta_2 - \delta_1) \cos(\phi_2 - \phi_1)}.$$

If one of the two amplitudes is small compared with the other, then A_{CP} will be small regardless of the values of the weak and strong phases. This is the

^aUsing the unitarity relationship $\alpha + \beta + \gamma = \pi$, any number of amplitudes with different strong phases can be written as the sum of two amplitudes with at most two different weak phases.

case for the decay $B \rightarrow K\pi$, which is dominated by a penguin diagram, and $B \rightarrow \pi^+\pi^0$, which is mediated by tree diagrams. In contrast one would expect a large CP-asymmetry for $B^0 \rightarrow \pi^+\pi^-$, unless there is dynamical suppression, since the tree and penguin amplitudes are of comparable size. When a B^0 decays to a self-conjugate final state, like $\pi^+\pi^-$, the value of A_{CP} is simply related to the parameter C describing direct CP-violation in the expression for the time-dependent asymmetry, see Sec. 8.

2. Theoretical Overview

The theoretical problem to be solved is how to calculate the branching fractions and CP-asymmetries for the decay of a B meson to a hadronic final state. For many years the more common two-body and quasi-two-body decays have been understood qualitatively in terms of naïve factorization. Here, the leading quark from the B meson decay is assumed to be in one quark, while the second meson contains the spectator quark. The interaction is calculated using leading-order diagrams only, and the two quarks are assumed to propagate independently of each other. Predictions for BF are made, but without control over, or understanding of, systematics, and all values for A_{CP} are, of course, identically zero. Although useful as a guide to experimental measurements, a major drawback of naïve factorization is its lack of any sound theoretical basis.

2.1. QCD Factorization (QCDF)

Any attempt to calculate BF and A_{CP} from first principles, using QCD, must take into account non-perturbative effects relating mesons to quarks and gluons, higher-order terms resulting from the low energy scale of the interaction, and long-range interactions that are not amenable to a perturbative approach. Such QCD calculations are based on a low-energy effective Hamiltonian written as the sum of generic amplitudes, which are classified as tree-like, penguin-like, electroweak and annihilation. QCD factorization,^{1,2} which relies on color transparency and the smallness of the parameter Λ_{QCD} compared with the mass of the B meson, m_B , enables a major simplification of the problem, since the amplitudes of the Hamiltonian factorize to leading order in Λ_{QCD}/m_B and all orders of perturbation theory.

Calculations are done to leading order in Λ_{QCD}/m_B , with non-factorizable corrections calculated to second order in α_S ; final-state interactions (FSI) and annihilation contributions are estimated in a model-dependent way. A nice feature of QCDF is that naïve factorization is recovered to leading order in α_S . CP-asymmetries arise naturally from the interference of (leading-order) tree and (second-order) penguin diagrams, with important modifications to the calculated values of branching fractions in some cases.

QCD factorization can be visualized diagrammatically as shown in Fig. 1 where the soft (form-factor and meson-formation amplitudes) and hard-scattering terms factorize. The lower, left-hand diagram represents the two combinations with m and M interchanged. An important feature of QCDF is that interactions between the two-meson systems are dominated by hard gluon exchange, and not soft processes, as shown in the right-hand lower diagram of Fig. 4.

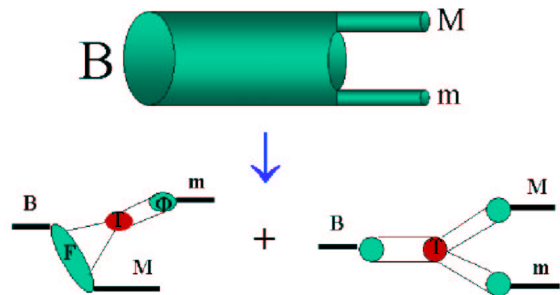


Figure 1. Visualising QCD Factorization in the decay of a B meson to two charmless mesons: M and m . T represents the hard-scattering kernel, F the semi-leptonic form factor and Φ the leading-twist light-cone distribution amplitudes.

One of the important results of QCDF is that the strong phase difference, between tree and penguin diagrams for example, is generally small, and this leads to predictions of small values for A_{CP} . Predictions of BF and A_{CP} are currently made for pseudoscalar-pseudoscalar (PP) and pseudoscalar-vector (PV) mesons. The major thrust of the theory is to calculate the angles α and γ of the unitarity triangle, using a subset of decays where model-dependent effects are well under control. There are significant concerns in applying QCDF to all rare decays, and hence searching for new physics, since it is not clear whether m_B is large enough compared with

Λ_{QCD} for the leading-order expansion to be valid, and whether the model-dependent annihilation terms are small enough to be under control in the calculations.

2.2. Flavor $SU(3)$ Symmetry

An alternative approach to the calculation of BF and A_{CP} for rare and unmeasured processes is to use experimental input from selected final states, each having one dominant (hard-scattering) amplitude, to estimate the amplitudes contributing to the rare process. For example the BF for the decay $B \rightarrow \pi^+\pi^0$ ($\pi^+\omega$) determines the amplitude for the tree diagram in non-strange PP (PV) final states, while that for $B \rightarrow \pi^+K^0$ determines the penguin amplitude for strange PP final states. Using flavor $SU(3)$ symmetry^{3,4,5} the tree and penguin amplitudes for strange and non-strange PP and PV final states can then be related to each other, as for example:

$$\left|\frac{p}{p'}\right|^2 = \left|\frac{V_{td}}{V_{ts}}\right|^2 = 0.039; \left|\frac{t}{t'}\right|^2 = \left|\frac{V_{us}}{V_{ud}}\right|^2 \left|\frac{f_K}{f_\pi}\right|^2 = 0.076$$

where p and t represent the penguin and tree amplitudes, respectively, with the primes corresponding to the final state having a strange meson. Electroweak and annihilation contributions, as well as the strong phase difference between dominant hard-scattering diagrams, are then included in such a way as to give the best fit to the more common BF. Such an approach is illustrated in Fig. 2, where the contributions from the soft (non-perturbative) processes are effectively treated as constants subsumed in the measured BF.

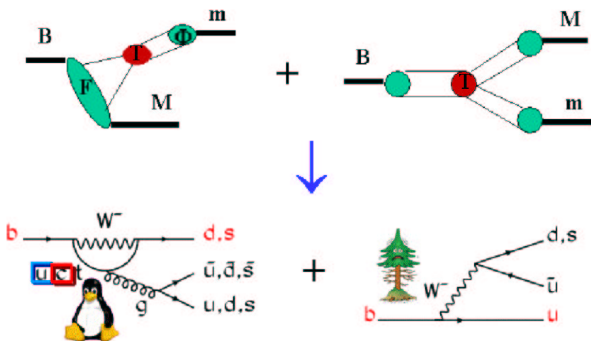


Figure 2. Pictorial representation of phenomenological approaches to B decay such as $SU(3)$ flavor symmetry.

This approach has the enormous merit of classifying and relating measured branching fractions and asymmetries in addition to predicting values for as-yet-unmeasured ones. It gives experimentalists a useful tool in searching for inconsistencies in data and looking for effects that may be due to physics beyond the Standard Model.

2.3. Model-Independent Calculations

In the event of any significant disagreement between a measured quantity, confirmed by a second experiment, and a theoretical prediction based on the Standard Model, attention would most likely be focused on the assumptions, approximations and model dependence of the calculations before claiming new physics. It would then be advantageous to consider calculations based only on isospin and $SU(3)$, which are less susceptible to dynamical assumptions. One useful class of such calculations includes the Grossman-Quinn bound⁶ and succeeding work,⁷ which put limits on possible deviations from simple expectations of the Standard Model calculations of CP-asymmetries.

3. Signal Selection and Background Rejection

When an $\Upsilon(4S)$ is produced in an e^+e^- collision it decays into a pair of B mesons described by a coherent, two-body wave function. At the instant one B decays the other has the opposite flavor. Hence by determining the flavor of one B the other may be tagged, which is essential for the study of neutral final states such as ϕK_s . Tagging and vertex reconstruction are studied using large data samples, where one B meson is a fully reconstructed final state. This minimizes the error from these sources entering the analysis of the small signals from the rare decay processes under study. Two invariant quantities are used to select signal events, m_{ES} the beam energy substituted mass peaking at the B mass, and ΔE the missing energy peaking at zero, defined as:

$$m_{ES} = \sqrt{(E_{beam}^*)^2 - p_B^{*2}}$$

$$\Delta E = E_B^* - E_{beam}^*$$

where p_B and E_B are the momentum and energy of the B meson, E_{beam} the energy of the beam and the

asterisk denotes the center-of-mass system. The resolution of m_{ES} is dominated by that of the beam energy and is about 3 MeV for all processes, while the resolution for ΔE depends on the final state but is typically 20 - 30 MeV. Energy resolution is among the many quantities studied by Monte Carlo (MC) simulation, with any small deficiencies in the behaviour of the MC being corrected from the comparison of MC and data for high statistics control samples. Some discrimination against background is given by the dependence of ΔE on the particle types in the final state. Figure 3 shows the experimental data for the control sample $B^0 \rightarrow D^- \pi^+$ compared with the two MC distributions $D^- \pi^+$ and $D^- K^+$, where the misidentification of the π^+ with a K^+ causes a shift in the ΔE distribution.

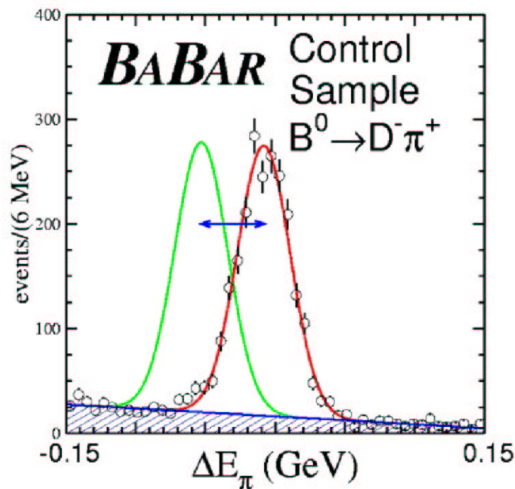


Figure 3. Distribution of ΔE for the control sample $B^0 \rightarrow D^- \pi^+$, shown as points with error bars. The curve centred at zero is expected for the correct identification of the bachelor pion, that offset to negative values for the pion misidentified as a kaon.

The dominant source of background in the rare-signal channels arises from the random combinations of particles in continuum events, which happen to satisfy energy and momentum conservation for fake B decays. Since B mesons are produced almost at rest in the center-of-mass they decay rather isotropically, whereas continuum events are produced in narrow, back-to-back jets aligned with the beam axis. Discrimination against background therefore relies on the different angular properties for production and decay of the real and fake B mesons. After preliminary cuts to remove the bulk of the background

with little loss of signal, the angular information for the remaining data sample is combined into a Fisher discriminant, F . The signal and background probability distributions for F , m_{ES} and ΔE are then used in the likelihood fit, together with particle-identification (PID) information, to identify the signal sample. The power of a Čerenkov detector to identify particle types and discriminate signal from background is illustrated in Fig. 4, where a sample of events containing a proton or antiproton is cleanly separated from the rest. BaBar relied on this to set the very small upper limit:⁸

$$BF(B^0 \rightarrow \bar{p}p) < 2.7 \times 10^{-7} (90\% \text{C.L.}).$$

The majority of information on baryonic final states has so far been produced by CLEO and Belle,⁹ with evidence for the first two-body baryonic B decay presented at EPS¹⁰ by Belle with the measurement:

$$BF(\bar{B}^0 \rightarrow \Lambda_c^+ \bar{p}) = (2.19_{-0.49}^{+0.56} \pm 0.32 \pm 0.57) \times 10^{-5}.$$

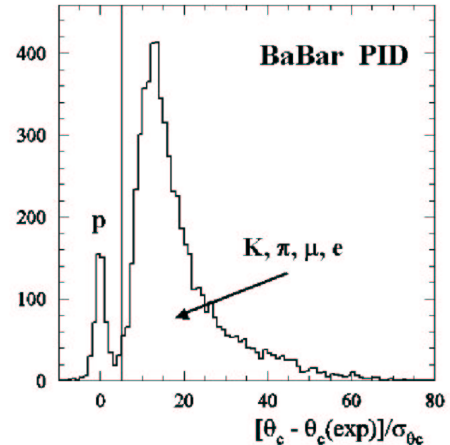


Figure 4. Separation of protons from other particles using angular information from the BaBar DIRC Čerenkov detector. The distribution shows the number of events as a function of the number of standard deviations by which the measured Čerenkov angle differs from that expected for a proton.

4. BF and A_{CP} for $K\pi$, $\pi\pi$ and KK

A summary of branching fractions for $K\pi$, $\pi\pi$ and KK final states^{11,9} is given in Table 1. Of particular note is the measurement of $B^0 \rightarrow \pi^0 \pi^0$. From a sample of 140 fb^{-1} ($1.52 \times 10^8 B\bar{B}$) Belle have a signal of 26 ± 9 events,¹² with a statistical significance of 3.4σ , while BaBar have a signal of $46 \pm 13 \pm 3$ events¹³ from 113 fb^{-1} and quote an overall significance of 4.2σ . Also noteworthy is the significant

Table 1. Summary of branching fractions in units of 10^{-6} for $K\pi$, $\pi\pi$ and KK final states.

Mode	BaBar	Belle	CLEO	Average
$K^+\pi^-$	17.9 ± 1.1	18.5 ± 1.2	18.0 ± 2.6	18.2 ± 0.8
$K^0\pi^+$	22.3 ± 2.0	22.0 ± 2.2	18.8 ± 4.3	21.8 ± 1.4
$K^+\pi^0$	12.8 ± 1.6	12.8 ± 1.8	12.9 ± 2.7	12.8 ± 1.1
$K^0\pi^0$	11.4 ± 1.9	12.6 ± 22.8	12.8 ± 4.3	11.9 ± 1.5
$\pi^+\pi^-$	4.7 ± 0.6	4.4 ± 0.7	4.5 ± 1.5	4.6 ± 0.4
$\pi^+\pi^0$	5.5 ± 1.2	5.3 ± 1.4	4.6 ± 19	5.3 ± 0.8
$\pi^0\pi^0$	2.1 ± 0.7	1.7 ± 0.7	< 4.4	1.9 ± 0.5
K^+K^-	< 0.6	< 0.7	< 0.8	< 0.6
K^+K^0	< 2.5	< 3.4	< 3.3	< 2.5
K^0K^0	< 1.8	< 3.2	< 3.3	< 1.8

increase in precision of the measurements since the publication of PDG 2002.¹⁴

Since the decay of a B to $K\pi$ or $\pi\pi$ usually proceeds through both penguin and tree diagrams, there is a significant dependence of the BF for many of the decay modes on the angle γ of the unitarity triangle. Ratios of BF calculated with QCDF (Fig. 14¹) were in reasonable agreement with the data in 2001 for a value of γ around 75° and remain so despite the increase in precision of the measured quantities. However, the calculated BF of $(0.2 - 0.5) \times 10^{-6}$ is in disagreement with the measured BF of $(1.9 \pm 0.5) \times 10^{-6}$ for the decay $B^0 \rightarrow \pi^0\pi^0$. Arising from a color-suppressed diagram, the $\pi^0\pi^0$ BF is not easily amenable to calculation within the framework of QCDF and the authors claim that this result does not discredit the theory. It is worth noting that pQCD predicts an equally small value for the $\pi^0\pi^0$ BF,¹⁵ whereas the other $K\pi$ and $\pi\pi$ branching fractions agree reasonably with the experimental data.

By writing the magnitude of the amplitude as proportional to the square root of the BF, it is apparent that the isospin relationship for $B \rightarrow \pi\pi$

$$\sqrt{2}A(\pi^+\pi^0) - A(\pi^+\pi^-) = \sqrt{2}A(\pi^0\pi^0)$$

is satisfied by the experimental data. This is to be expected, since isospin conservation is good to 1-2% in strong interactions, and the expected contribution from electroweak processes is not expected to be greater than about 2%.¹⁶ Using SU(3) arguments in addition to isospin, the following two ratios of BF are expected to be equal¹⁷ so long as the electroweak

Table 2. Average CP-asymmetries (%) for Belle and BaBar data¹¹ compared with predictions from pQCD¹⁶ and QCDF.¹

Mode	A_{CP} (Expt)	A_{CP} (pQCD)	A_{CP} (QCDF)
$K^+\pi^-$	-9 ± 3	$-13 \leftrightarrow -22$	$+5 \pm 10$
$K^0\pi^+$	-1 ± 6	$-0.6 \leftrightarrow -1.5$	0 ± 1
$K^+\pi^0$	0 ± 7	$-10 \leftrightarrow -17$	$+7 \pm 10$
$K^0\pi^0$	3 ± 37		-3 ± 4
$\pi^+\pi^-$		$16 \leftrightarrow 30$	-6 ± 13
$\pi^+\pi^0$	-7 ± 14	0	-2 ± 5
$\pi^0\pi^0$			45 ± 60

penguin contribution can be neglected:

$$R_{Neut} = \frac{BF(B^0 \rightarrow K^+\pi^-)}{2BF(B^0 \rightarrow K^0\pi^0)} = 0.77 \pm 0.10$$

$$R_{Chg} = \frac{2BF(B^+ \rightarrow K^+\pi^0)}{2BF(B^+ \rightarrow K^0\pi^+)} = 1.17 \pm 0.13.$$

The difference of (0.40 ± 0.16) is not significant, and it will be interesting to see whether the two ratios change with an increase in data.

A comparison of the theoretical predictions for A_{CP} with data is of some interest, since the asymmetries arise as a consequence of the interference of different contributing amplitudes and are zero at leading order. Table 2 shows that most asymmetries are predicted to be small, and are in agreement with data. As yet there is no claimed observation of a non-zero asymmetry, which would indicate direct CP-violation, but the data for $K^+\pi^-$ is tantalizingly

Table 3. Branching fractions (10^{-6}) for data compared with predictions from pQCD.

	Data	pQCD
K^+K^-	< 0.6	0.05
K^+K^0	< 2.5	1.7
K^0K^0	< 1.8	1.8

close with measurements of:

$$A_{CP} = (-8.8 \pm 3.5 \pm 1.8)\% \quad (\text{Belle}^{18})$$

$$A_{CP} = (-10.7 \pm 4.1 \pm 1.2)\% \quad (\text{BaBar}^{19}).$$

It is of some interest that pQCD and QCDF predict asymmetries with opposite signs, although the theoretical uncertainties may be too large for this ever to become a significant issue.

CDF has evidence for the decays $B_d \rightarrow \pi^+\pi^-$ and $K^+\pi^-$, as well as $B_s \rightarrow K^+\pi^-$ and K^+K^- .²⁰ All four decays populate the same mass window (Fig. 5) and are untangled using a combination of dE/dx and the different division of momentum between the particles in the four final states.

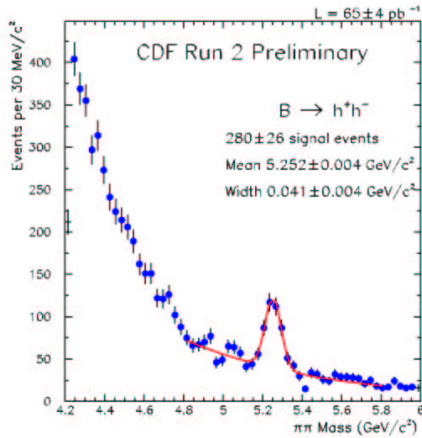


Figure 5. Invariant mass of two charged hadrons, each assumed to be a pion, showing a peak at the B mass in the CDF experiment.²⁰

After untangling the samples, the CP-asymmetry for $B_d \rightarrow K\pi$ is calculated to be $A_{CP} = (2 \pm 15 \pm 2)\%$, based on 39 ± 14 events, which is in good agreement with results from Belle and BaBar. Rescattering could modify the BF and CP-asymmetries for $K\pi$ and $\pi\pi$ final states, which in turn would complicate the extraction of the unitarity angles γ and α . If it were significant, it might be expected to increase the BF into KK through intermediate DD or

Table 4. Branching fractions (10^{-6}) and CP-asymmetries (%) for B decays to pseudoscalar-vector particles for BaBar²¹ and Belle.²²

Mode	BF	BF	A_{CP}	A_{CP}
	(BaBar)	(Belle)	(BaBar)	(Belle)
$\rho^+\pi^-$	22.6 ± 2.8	29.1 ± 6.4	-11 ± 7	-38 ± 21
ρ^+K^-	7.3 ± 1.8	15.1 ± 4.1	19 ± 18	22 ± 23
$\rho^0\pi^0$	< 2.5	6.0 ± 3.1		
$\rho^+\pi^0$	11.0 ± 2.7		23 ± 17	
$\rho^0\pi^+$	9.3 ± 1.3	8.0 ± 2.3	-17 ± 11	
ρ^0K^+	3.9 ± 3.7	3.9 ± 1.0		
ωK^0	5.3 ± 1.4	4.0 ± 2.0		
ωK^+	5.0 ± 1.1	6.7 ± 1.4	-5 ± 16	6 ± 20
$\omega\pi^0$	< 3	< 1.9		
$\omega\pi^+$	5.4 ± 1.1	5.7 ± 1.5	4 ± 17	48 ± 23

$\pi\pi$ states. Current BF for KK , shown in Table 3, have upper limits consistent with predictions from pQCD, so that there is no evidence for rescattering.

5. BF and A_{CP} for $\rho\pi$, ρK , $\omega\pi$ and ωK

Branching fractions and asymmetries for B decays to $\rho\pi$, ρK , $\omega\pi$ and ωK are shown in Table 4. The recent results for $B^0 \rightarrow \rho^0\pi^0$ from Belle and BaBar are consistent, but it is too early to say with confidence what the BF is and whether it is small enough to reduce uncertainties in the extraction of α from the $\rho\pi$ final states. It might be expected from a simple consideration of the contributing diagrams that the BF for ωK would be considerably larger than that for $\omega\pi$; it is not, and we return to this in more detail later.

6. Dalitz Plot Analyses of $K\pi\pi$ and KKK

Understanding the resonance contributions to a three-body final state requires an analysis of the Dalitz plot. With 56.4 fb^{-1} BaBar have made an approximate analysis of the decay $B^+ \rightarrow K^+\pi^+\pi^-$ by concentrating on the resonant bands for the $K^*(890)$ and higher-mass K^* , as well as $\rho(770)$, $f_0(980)$ and χ_c . Interference cannot be taken into account in this approach, and to reduce the effects from the domi-

Table 5. Branching fractions (10^{-6}) for contributions to the $K^+\pi^+\pi^-$ (upper 10 rows) and $K^+K^+K^-$ Dalitz plot (lower 5 rows) for recent BaBar²³ and Belle²⁴ data, with average values for all data.⁹ The BF for $K^+f_0(980)$ and $K^+\chi_c(3400)$ include the BF of the resonance to $\pi^+\pi^-$ or K^+K^- as appropriate.

Mode	BaBar	Belle	Average
$K\pi\pi)_{Total}$	59 ± 5	46 ± 5	52.2 ± 3.5
$K\pi\pi)_{NonRes}$	< 17	14 ± 6	
$K^{*0}(890)\pi^+$	15.5 ± 4.4	8.5 ± 1.5	9.0 ± 1.3
$K^{*0}(1400)\pi^+$		40.3 ± 6.5	40.3 ± 6.5
$K^{*0}(1430)\pi^+$		< 10.5	< 10.5
$K^{*0}(1689)\pi^+$		< 21	< 21
$K^+\rho(770)$	3.9 ± 3.7	3.9 ± 1.0	4.1 ± 0.9
$K^+f_0(980)$	9.2 ± 2.9	10.3 ± 2.4	9.9 ± 1.9
$K^+f_2(1270)$		< 6.3	< 6.3
$K^+\chi_c(3400)$	1.46 ± 0.37	1.17 ± 0.42	
$KKK)_{Total}$	29.6 ± 2.6	29.4 ± 2.4	29.5 ± 1.8
$KKK)_{NonRes}$		22.5 ± 4.9	
$K^+\phi(1020)$	10.0 ± 1.0	8.6 ± 1.1	9.0 ± 0.7
$K^+f_2(1525)$		< 12.8	< 12.8
$K^+\chi_c(3400)$		0.85 ± 0.29	

nant D^0 , J/Ψ and Ψ' resonances, the overlap region is removed. The branching fractions of the resonant contributions are given in Table 5. Using the larger data sample of 140 fb^{-1} , Belle have made an amplitude analysis of both the $K^+\pi^+\pi^-$ and $K^+K^+K^-$ Dalitz plots, having totals of 2584 and 1400 events, respectively. The background arising from continuum processes is fitted (with high precision) using sideband samples with several times the number of non-signal events than is contained in the Dalitz plot. The background amplitude is parameterized with the following function, which takes into account resonant contributions from $K^*(890)$ and $\rho(770)$ as well as a non-resonant term, which is a function of the invariant mass-squares, s_{ij} , of the two-particle combinations.

$$A_{BG} = \sum_k \alpha_k e^{-\beta s_{ij}} + BW(K^*) + BW(\rho)$$

The signal amplitude is fitted to a sum of resonant (Breit-Wigner) terms and a non-resonant, non-phase-space-like term. For the $K^+\pi^+\pi^-$ analysis the

masses and widths are fixed for $K^*(890)$, $K^*(1400)$, $\rho(770)$, $\chi_c(3400)$ and left floating for $f_0(980)$ and a broad distribution described as $X(1350)$; for the $K^+K^+K^-$ analysis the masses and widths are fixed for $\phi(1020)$ and $\chi_c(3400)$ and left floating for the broad distribution described as $X(1500)$. The signal amplitude is described as:

$$A_{Signal} = \sum_R \alpha_R e^{i\delta_R} + \left(\frac{a_1}{s_{12}^{p_1}} e^{i\phi_1} + \frac{a_2}{s_{23}^{p_2}} e^{i\phi_2} \right)_{NonRes}$$

where the parameters a_R , δ_R , p_1 , p_2 , ϕ_1 and ϕ_2 are varied to give the best overall fit to the Dalitz plot.

The quality of the fit to the Dalitz plot is appreciated best from the projected fits of invariant mass and helicity for the two-body combinations. Figure 6 shows these for the $K\pi$ and $\pi\pi$ combinations. As expected, the helicity distributions are well described by spin-1 (spin-0) in the vicinity of the $K^*(890)$ ($f_0(980)$) mass regions. The BF for the different contributions to the $K\pi\pi$ and KKK Dalitz plots, together with the total and non-resonant contributions, are given in Table 5.

Despite the excellent fit, the non-phase-space, non-resonant contribution to the Dalitz plot is a cause for concern, since it is not understood. The values of the BF from both BaBar and Belle must therefore be treated with caution at the present time.

7. $B \rightarrow VV$ and Longitudinal Polarization

In addition to branching fractions and CP-asymmetry, a measurement of the angular distribution of the two mesons enables further tests of theoretical predictions. Two complementary decompositions can be used: orbital angular momentum states S, P and D, or a longitudinal and two transverse polarization states. In the latter case the longitudinal polarization is a CP-even state while the transverse polarization is mixed, with both CP-odd and CP-even components. On the basis of helicity arguments, assuming short-distance dominance within the framework of perturbative QCD, the longitudinal polarization, f_L , is predicted to be:²⁵

$$f_L = 1 - \mathcal{O}(m_V^2/m_B^2)$$

where m_V is the mass of one of the vector mesons. Thus, for decays of a B meson into two mesons of the type ρ , η , ψ or K^* the expectation for f_L is in the region of 95 – 99%. There are no simple predictions

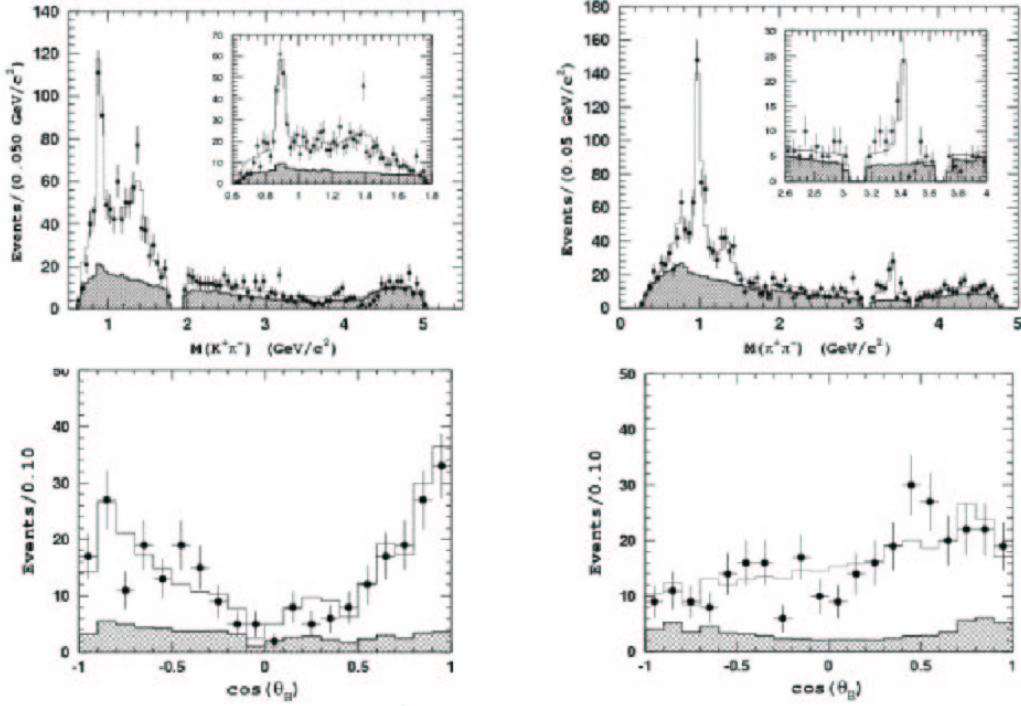


Figure 6. Projections of the $K\pi\pi$ Dalitz plot onto $K\pi$ (left) and $\pi\pi$ (right) showing the mass spectrum (upper) and helicity distribution (lower). The background contribution is shown hatched in all plots. The inset plots show the mass regions around the K^* and χ_C in more detail. The open histogram shows the overall fit to be compared with the data points shown with error bars. The helicity distributions are plotted for a mass interval around the K^* and f_0 , respectively, for the $K\pi$ and $\pi\pi$.

for the transverse components, which are expected to be small and will be very difficult to measure with any reasonable precision. The angular distribution used to measure f_L is given by

$$\frac{1}{\Gamma} \frac{d^2\Gamma}{d\cos\theta_1 d\cos\theta_2} = \frac{1}{4} (1 - f_L) \sin^2\theta_1 \sin^2\theta_2 + f_L \cos^2\theta_1 \cos^2\theta_2$$

where θ_1 and θ_2 are the helicity angles of the decay products of the two vector mesons. For example, in the decay $B \rightarrow \rho^+\rho^-$, then θ_1 would be the angle between the momentum vector of the π^+ and that of the ρ^+ , both measured in the rest frame of the ρ^+ .

7.1. $B \rightarrow \rho\rho$ and ρK^*

Measurements of branching fractions, CP-asymmetries and longitudinal polarizations for the final states $\rho^0\rho^0$, $\rho^+\rho^-$, $\rho^+\rho^0$ and $\rho^0 K^{*+}$ are given in Table 6. A projection of the $\rho^+\rho^-$ onto the π^+ helicity axis is shown in Fig. 7. The structure in the background (dotted curve) under the signal arises from the variation in acceptance.

The observation of $\rho^+\rho^-$ at more than 5σ overall

Table 6. Measurements of branching fraction, CP-asymmetry and longitudinal polarization from BaBar²⁶ and Belle²⁷ for $\rho\rho$ and ρK^* final states. All data are from BaBar, alone, except for $\rho^+\rho^0$.

	BF (10^{-6})	A_{CP} (%)	f_L (%)
$\rho^0\rho^0$	< 2.1		
$\rho^+\rho^-$	27 ± 9		99 ± 8
$\rho^+\rho^0$	23 ± 8	-19 ± 23	97 ± 8
Belle	32 ± 10	0 ± 22	95 ± 11
$\rho^0 K^{*+}$	11 ± 4	20 ± 32	96 ± 16

significance, completes the measurement of the $\rho\rho$ final states. All values of longitudinal polarization shown in Table 6 are in agreement with theoretical expectation, and the values of A_{CP} are consistent with zero.

The $\rho\rho$ system is an isospin triplet like the $\pi\pi$ system, and hence the following relationship should hold good:

$$\sqrt{2}A(\rho^+\rho^0) - A(\rho^+\rho^-) = A(\rho^0\rho^0)$$

where A is the amplitude for the decay $B \rightarrow \rho\rho$. Using the values from Table 6 gives a value for the LHS of (2.1 ± 1.3) , to be compared with < 2.1 for the RHS, where the square root of the BF has been used for each amplitude, and the weighted-average BF for the $\rho^+\rho^0$ was used. Although not inconsistent, the situation is uncomfortable. An optimistic possibility is that the true value for $B(\rho^0\rho^0)$ might turn out to be smaller than presently measured, but it is also possible that there will be adjustments to the BF of either $\rho^+\rho^-$ or $\rho^+\rho^0$, the final states with neutral pions, which are more difficult to distinguish from background.

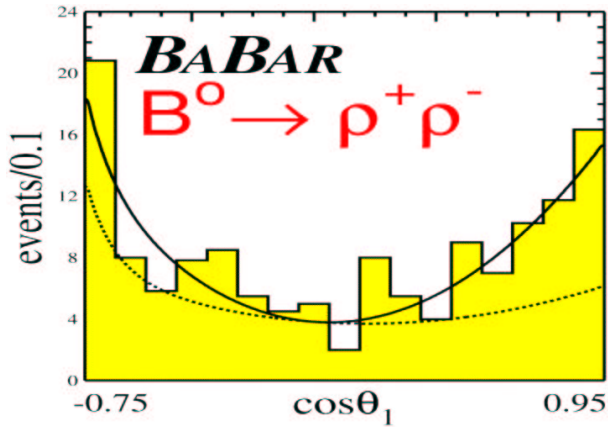


Figure 7. The projected helicity distribution, solid curve, of the π^+ from the fit to the combined angular distribution is compared with the total data sample, histogram. The dotted curve shows the background.

7.2. Bounds on α from $B \rightarrow \pi\pi$ and $\rho\rho$

The similarity between the $\pi\pi$ and $\rho\rho$ systems, both consisting of identical bosons of isospin $I = 1$, suggests that one might apply the Grossman-Quinn bound⁶ in order to obtain a limit on the difference between the measured unitarity angle, α_{Eff} , and the true angle α . The relationship gives:

$$\sin^2(\alpha - \alpha_{eff}) < \frac{BF(B^0 \rightarrow \rho^0\rho^0)}{BF(B^0 \rightarrow \rho^+\rho^-)} < 0.10$$

leading to a limit on $|\alpha - \alpha_{Eff}|$ of approximately 20° at 90% CL,²⁶ compared with approximately 50° for the $\pi\pi$ case. The value is so large for the $\pi\pi$ system as to be of no practical use, whereas the limit on the $\rho\rho$ system – if valid – is of very great interest.

However, the differences between the $\pi\pi$ and $\rho\rho$ systems require some discussion before this bound can be accepted. First, pions are pseudoscalar mesons of definite mass, whereas the ρ is a vector meson with a substantial width. Here, the experimental finding is that the longitudinal polarization is consistent with 100%. This is very important, since it indicates that the $\rho\rho$ system may be described as $\rho_L\rho_L$ – a pure CP-even state, just like the two-pion system. Also, Bose-Einstein statistics would require that a pure $\rho\rho$ system had no contribution from isospin $I = 1$, which is an important condition for the Grossman-Quinn bound to apply. The concern, which is currently receiving a good deal of thought, is to what extent modifications from final-state interactions and the presence of non-resonant background are understood well enough to be taken into account in the analysis.

7.3. Vector and Scalar Couplings

It was mentioned earlier that the branching fractions for ωK and $\omega\pi$ are very similar, with a ratio of 0.9 ± 0.3 , whereas on the basis of CKM couplings one would expect the BF for ωK to be much larger than that for $\omega\pi$. Another situation, where simple expectation is confounded, occurs in the comparison of decays to final states $(K^0\pi^+, K^{*0}\pi^+)$ and $(\pi^+\pi^0, \pi^+\rho^0, \rho^+\rho^0)$.

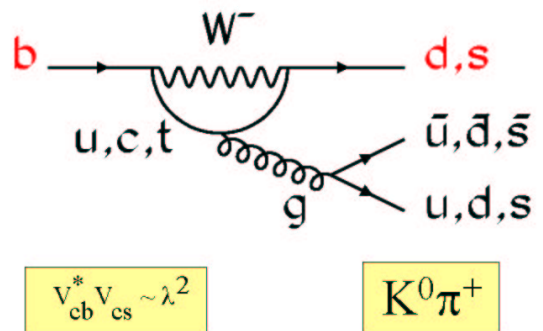


Figure 8. Penguin graph describing $B^+ \rightarrow K^0\pi^+$ and $K^{*0}\pi^+$. The dominant contribution is for the c quark coupling to the b and s quarks.

The $K\pi$ decays are dominated by the penguin diagram of Fig. 8, where the neutral kaon includes the leading s quark. Within corrections of 30 - 40%

arising from uncertainties in the form factors, the BF for $K^{*0}\pi^+$ and $K^0\pi^+$ might be expected to be in the ratio of the square of the decay constants, namely 1.85. Experimentally, however, the ratio is very different at 0.65. The decays $\pi^+\pi^0$, $\pi^+\rho^0$ and $\rho^+\rho^0$ are mediated by the tree diagram of Fig. 9, where the leading quark is in the charged meson. Their BFs would be expected to be in the ratio 1: 2.6: 4.4, which agree much better with the experimental ratios of 1: 1.7: 5.0 than those for $K\pi$. It might be thought that the vector boson (W or g) would couple more strongly to a vector meson, and hence an enhancement occur for K^* and ρ production, but the opposite is true for $K^{*0}\pi^+$ and $K^0\pi^+$, while there seems to be little effect for the $\pi^+\pi^0$, $\pi^+\rho^0$ and $\rho^+\rho^0$ decays. Thus, there seems to be no discernible pattern to this behavior.

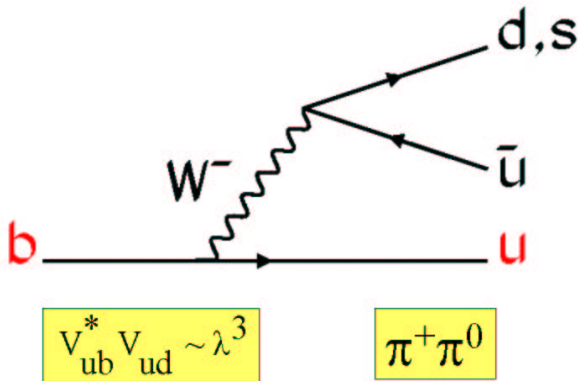


Figure 9. Tree diagram for the decays $B^+ \rightarrow \pi^+\pi^0$, $\pi^+\rho^0$ and $\rho^+\rho^0$.

Returning to the consideration of CKM factors, it might be expected that decays mediated by the tree diagram of Fig. 9 would be greatly suppressed relative to those mediated by the penguin diagram of Fig. 8, since the relative CKM factor is $\lambda^2 \approx 0.05$. The experimental ratios R_{Exp} , shown in Table 7, do not indicate such a suppression, and it is clear that an additional enhancement of (approximately) a factor of 10 to the naïve theoretical ratios R_{Th} must occur. This suggests that the ratio of the penguin to tree amplitudes is about 0.3, a value which seems to hold widely in B decays.

In conclusion, a simple pictorial understanding of branching fractions can be misleading, and it is necessary to refer to fundamental theoretical calcu-

Table 7. Ratios of branching fractions from experimental measurements (R_{Exp}) and simple theoretical considerations (R_{Th}) based on CKM factors and decay constants (f_{decay}).

Mode	CKM	$(f_{decay})^2$	R_{Th}	R_{Exp}
$K^0\pi^+$	1	1	1	1
$K^{*0}\pi^+$	1	1.85	1.85	0.65
$\pi^+\pi^0$	λ^2	0.66	0.03	0.27
$\pi^+\rho^0$	λ^2	1.71	0.085	0.46
$\rho^+\rho^0$	λ^2	4.4	0.22	1.35

lations for a quantitative explanation.

7.4. The Decays $B \rightarrow \phi K$ and ϕK^*

The final states ϕK (Fig. 10) and ϕK^* are produced through a single penguin diagram, similar to Fig. 8, where the b quark decays to an s quark and the gluon couples to an $s\bar{s}$ pair, to form a ϕ containing the leading s quark and a K or K^* which includes the spectator quark together with an s quark from the gluon. The dominance of this single diagram means that the branching fractions for all four charged and neutral final states (Table 8) are expected to be equal, within corrections due to different decay constants and form factors, and their CP-asymmetries close to zero. A glance at Table 8 shows that these expectations are met. For completeness we note that CDF see a signal in the decay $B^+ \rightarrow \phi K^+$, which they translate into a branching fraction³⁰ of $(6.9 \pm 2.1 \pm 0.8) \times 10^{-6}$ by normalization with the known BF for $J/\Psi K^+$.

However, the measured values of longitudinal polarization for the two vector-vector final states are completely at variance with the expectation of (approximately) 100%. This is not yet understood. It may be an indication for physics beyond the Standard Model in support of the anomalous value for $\sin(2\beta)$ in the channel $B^0 \rightarrow \phi K^0$ reported by Belle at this conference,³¹ or it could indicate a breakdown of factorization through the theoretical assumption that calculations to leading order in Λ_{QCD}/m_B are sufficient. Whatever the explanation, these decay modes are now of prime interest to experimentalists and theorists alike. Finally, we note that the small value for the upper limit of 4×10^{-7} (at 90% CL) for the branching fraction³² $B^+ \rightarrow \phi\pi^+$ gives no in-

Table 8. Branching fractions, CP-asymmetries and longitudinal polarization for the decay modes $B \rightarrow \phi K^0$, ϕK^+ , ϕK^{*0} and ϕK^{*+} as measured by BaBar²⁸ and Belle.²⁹

Mode	BF (10^{-6})		A_{CP} (%)		Polarization (%)	
	BaBar	Belle	BaBar	Belle	BaBar	Belle
ϕK^0	8.4 ± 1.6	9.0 ± 2.2				
ϕK^+	10.0 ± 1.0	8.6 ± 1.1	4 ± 9	1 ± 13		
ϕK^{*0}	11.2 ± 1.5	10.0 ± 1.8	4 ± 12	7 ± 16	65 ± 7	43 ± 10
ϕK^{*+}	12.7 ± 2.4	6.7 ± 2.2	16 ± 17	-13 ± 31	46 ± 12	

Table 9. Branching fractions (10^{-6}) and CP-asymmetries (%) for $B \rightarrow \eta K^{(*)}$ and $\eta' K^{(*)}$ decays from BaBar³³ and Belle.³⁴

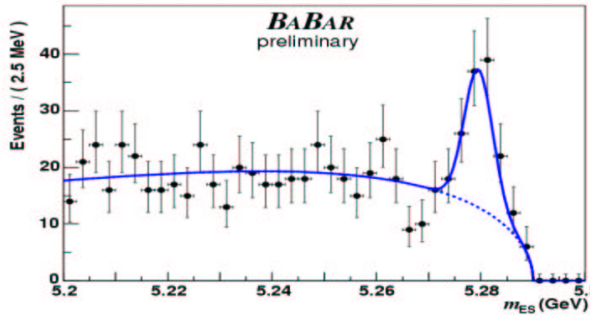


Figure 10. Invariant mass m_{ES} for the final state ϕK_s . The solid curve shows a projection of the likelihood fit for the event sample, with background described by the dotted curve.

Mode	Belle		BaBar	
	BF	A_{CP}	BF	A_{CP}
ηK^+	5.3 ± 1.9		2.8 ± 0.8	-32 ± 22
ηK^0			< 4.6	
$\eta' K^+$	78 ± 11	-2 ± 7	76.9 ± 5.6	4 ± 5
$\eta' K^0$	68 ± 13		60.6 ± 7.2	
ηK^{*+}	26.5 ± 8.4		25.7 ± 4.2	15 ± 14
ηK^{*0}	16.5 ± 4.8		19.0 ± 2.6	3 ± 11
$\eta' K^{*+}$	< 90		< 12	
$\eta' K^{*0}$	< 20		< 6.4	

dication of final-state interactions.

7.5. The Decays $B \rightarrow \eta K^{(*)}$ and $\eta' K^{(*)}$

The penguin graph of Fig. 11(a), which dominates the B decay to ϕK , might be expected to play a similar role in the decay to ηK final states, in which case branching fractions for ηK , ηK^* , $\eta' K$, and $\eta' K^*$ would all be expected to be equal within 20 - 30%. A glance at Table 9 shows that this expectation is not fulfilled.

Instead, branching fractions for ηK and $\eta' K^*$ are low by comparison with those for ϕK , while those for ηK^* and $\eta' K$ are significantly greater. A possible explanation for this discrepancy was given by Lipkin³⁵ several years ago. He pointed out that the penguin graph of Fig 11(b) also produces the ηK final states, and that if destructive interference between the amplitudes of Fig. 11(a) and (b) occurred for ηK then it would also occur for $\eta' K^*$, while constructive interference would occur for both $\eta' K$ and ηK^* . Only

recently have experimental measurements and theoretical calculations² become precise enough to test whether this explanation is sufficient, and it appears that an additional, flavor-singlet, penguin amplitude is necessary. Theoretical opinion is divided about the relative magnitude of this amplitude,^{2,5} but all agree that the CKM-suppressed contribution of Fig. 11 (c) is small, and therefore the charged and neutral final states should have very similar values of branching fractions. That does not appear to be the case and BFs for neutral modes do seem to be smaller than for charged ones, although the disagreement is not yet statistically significant.

Given the dominance of penguin graphs in the decay of B to ηK , one would expect all CP-asymmetries to be very small. Data as yet is sparse, but there is no indication in Table 9 of any non-zero values.

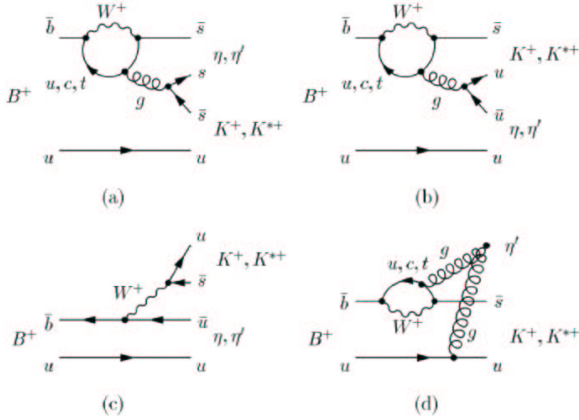


Figure 11. Feynman graphs contributing to the decay of a B meson to $\eta K^{(*)}$ and $\eta' K^{(*)}$ final states: a) Analogue of decay amplitude to ϕK ; b) Additional penguin amplitude which cannot occur for ϕK ; c) CKM-suppressed tree amplitude; d) Flavor-singlet penguin amplitude. All amplitudes contribute to charged final states, and all but (c) to neutral ones.

7.6. The Decays $B \rightarrow \eta^{(\prime)}\pi$ and $\eta^{(\prime)}\rho$

In principle, the Feynman graphs of Fig. 11 are also appropriate to the decays $B \rightarrow \eta^{(\prime)}\pi$ and $\eta^{(\prime)}\rho$, once all s quarks are replaced with d quarks – although no-one has yet suggested that a flavor-singlet penguin contribution is necessary. However, the relative magnitude of all penguin graphs is now reduced, and that of the tree amplitude increased, because of the changes in the CKM couplings. This means that in charged modes the effect of interference between penguin graphs (a) and (b) is likely to be reduced, while that between the tree and penguin amplitudes may become significant. These changes could give rise to large differences in branching fractions between the charged and neutral final states, and to measurable CP-asymmetries in charged final states, where both the tree and penguin amplitudes contribute.

Branching fractions and CP-asymmetries are shown in Table 10. BaBar has recently observed decays to the final states $\eta'\pi^+$, $\eta\rho^+$ and $\eta'\rho^+$, with combined statistical and systematic significances of 3.4, 4.8 and 3.8 sigma, respectively. Data on neutral decay modes is sparse, and it is not possible to draw any conclusions about the size of their BF's relative to charged ones. The ratio of $\eta\rho$ to $\eta\pi$ branching fractions is consistent with the expectation from decay constants, and the geometric-mean BF for $\eta\rho$ and $\eta\pi$ is about a factor of three smaller than that for $\eta^{(\prime)}K^{(*)}$. There is an indication of a non-zero

Table 10. Branching fractions (10^{-6}) and CP-asymmetries (%) for $B \rightarrow \eta^{(\prime)}\pi$ and $\eta^{(\prime)}\rho$ from BaBar³³ and Belle.³⁴

Mode	Belle		BaBar	
	BF	A_{CP}	BF	A_{CP}
$\eta\pi^+$	5.4 ± 2.1		4.2 ± 1.0	-51 ± 20
$\eta'\pi^+$	< 7		< 4.5	
$\eta\rho^+$	< 6.2		10.5 ± 3.4	6 ± 29
$\eta\rho^0$	< 5.5			
$\eta'\rho^+$			14.0 ± 5.4	
$\eta'\rho^0$	< 14			

CP-asymmetry for $\eta\pi^+$, which is not unexpected in light of the discussion above. It is of interest, however, that whereas a large asymmetry is predicted on phenomenological grounds, the same theoretical analysis⁵ predicts a small value of A_{CP} for $\eta\rho^+$. These are clearly interesting final states to monitor as statistics increase.

8. The Search for New Physics

Branching fractions for two-body final states are generally in good agreement with theoretical predictions, while measurements of the asymmetry are not yet precise enough to make rigorous tests. We saw earlier that the BF for $B^0 \rightarrow \pi^0\pi^0$ is significantly higher than the expectations from QCDF and pQCD, but theorists downplay this disagreement and are at pains to stress the difficulty of such color-suppressed calculations and of estimating theoretical errors. Of more significance is any difference between the measured and calculated ratio $B(B^0 \rightarrow \pi^0 K^0) / B(B^+ \rightarrow \pi^+ K^0)$. The QCDF calculation is very clean and gives a value of 0.40 ± 0.04 ,² compared with the measured ratio of 0.55 ± 0.08 . With a disagreement of less than two standard deviations there is no evidence for new physics.

There are still some worries about the calculations in QCDF of branching fractions for decays to the final states $\phi K^{(*)}$ and $\eta^{(\prime)}K^{(*)}$ where the values are generally lower than experimental measurements and subject to very large errors. One such comparison³⁶ of experimental and theoretical branching fractions and asymmetries has even sug-

gested that the model-dependent annihilation contribution may be too large for stable solutions to QCDF, and that the basic theoretical assumption of $\Lambda_{QCD}/m_B \ll 1$ is simply not true. Recent modifications to QCDF⁵ with a variety of choices of hadronic parameterizations have overcome this objection, but at the expense of weakening the predictive power. It therefore seems unlikely that new physics will be proclaimed on the basis of differences between measurements and QCD predictions, alone.

An alternative approach to the ground-up QCD calculations is to use minimal theoretical assumptions, such as isospin and flavor-SU(3) symmetry, in an attempt to put limits on possible uncertainties in calculations within the Standard Model. As an example, for all the decay modes $B^0 \rightarrow \phi K_s$, $\eta' K_s$ and $K^+ K^- K_s$ the time-dependent asymmetry is expected to have the form:

$$A(t) = S \sin(\Delta m t) + C \cos(\Delta m t)$$

where: $S = \sin(2\beta) + \Delta$, $C = \Delta$ and $\Delta = O(\lambda^2)$.

Given criteria for disagreement with the Standard Model, and hence claiming new physics – for example a five sigma difference between prediction and confirmed experimental measurements – the major question is the size of Δ . The origin of Δ is in the penguin loop of Fig. 12, where the b quark couples to the s quark via the exchange of a virtual W -boson and a u or c quark. The CKM parameters give the factor λ^2 , while the interaction amplitudes a^u and a^c , describing b to s quark coupling with the exchange of a u quark and c quark, respectively, are expected to be of similar size. Most theoretical calculations give values of Δ/λ^2 of 0.2 to 1, but an enhancement cannot be ruled out. A method of calculating an upper bound on Δ has been derived within the framework of isospin and SU(3)⁷ using ratios of branching fractions. A total of about 20 different branching fractions is used to bound Δ for the three final states [ϕK_s , $\eta' K_s$ and $K^+ K^- K_s$], with values of Δ ranging from 0.2 to 0.5. Although far too large currently to enable claims of physics beyond the Standard Model for these decays, the values of Δ are not dissimilar from the current experimental precision on S and C , and can be expected to decrease in a similar way as more data is accumulated.

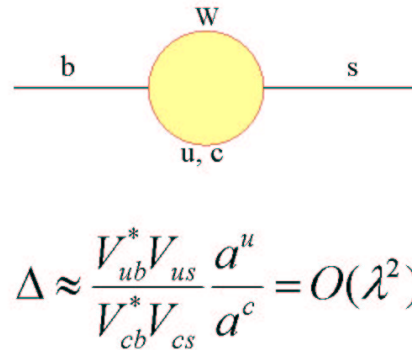


Figure 12. The origin of Δ in the penguin loop coupling the b and s quarks in the flavor-changing neutral decay of the B meson. The amplitudes a^u and a^c describe the dynamics of the quark interactions.

9. Summary and Outlook

The two B factories have made a major step forward in both the precision of measurements and in the wealth of new decay modes that have been analyzed. Real tests have become possible of factorization models and phenomenology. Indeed, theorists have been able to further our understanding of hadron dynamics and to build up a comprehensive picture of branching fractions in B decays, which enables physicists to look for inconsistencies in the experimental measurements of very rare decays. Measurements of CP-asymmetries are starting to become precise, and there is every hope that in the next year or two even more stringent tests of theory will become possible, since the predictions depend on our understanding of both the magnitudes and phases of the interfering amplitudes. In this respect, two final states to watch are $K^+ \pi^-$ and $\eta \pi^+$.

The relationship among the branching fractions of the decay modes $\eta^{(\prime)} K^{(*)}$ is now much better understood than it was two years ago thanks to very precise measurements and considerable theoretical progress both in QCDF and phenomenology. It is still unclear how important the di-gluon, flavor-singlet contribution is by comparison with the other two penguin graphs. Further progress needs a considerable reduction in theoretical uncertainties in the QCDF calculations, as well as an improvement in the precision of measured branching fractions. A major

puzzle in the strange final states is the anomalous value of the longitudinal polarization in the ϕK^* final state. A representative value of $(50 \pm 10)\%$ compared with the expectation of almost 100% indicates a worrying lack of theoretical understanding. It would be of real interest to measure the longitudinal polarization in other strange-particle final states to see whether the problem is associated with dominance of penguin graphs, compared with the tree graph for $\rho\rho$ final states.

The measurement of the branching fraction for $B^0 \rightarrow \pi^0\pi^0$ is an experimental triumph. It is surprising that the value is so much higher than previous theoretical estimates, but, as already mentioned, the theoretical calculations of such color-suppressed processes are extremely difficult. One of the unfortunate consequences of this (comparatively) large branching fraction is that its use via the Grossmann-Quinn relationship to limit the theoretical uncertainty on the unitarity angle α is diminished to the point of being useless. By contrast the situation with respect to $\rho\rho$ final states is very encouraging. The time-dependent analyses of $\rho^+\rho^-$ are soon expected to give values of α_{Eff} . Moreover, an improved measurement of the branching fraction for $\rho^0\rho^0$ will enable the difference between the measured and true values of α to be determined more precisely than the current upper limit of about 20° . Together, these measurements will provide an exciting new constraint on the determination of the (ρ,η) apex of the unitarity triangle.

Progress is being made in refining the criteria for claiming new physics on the basis of disagreement with the predictions of the Standard Model. Using measured branching fractions, limits have been calculated on the possible modification to the time-dependent asymmetry parameters for final states ϕK_s , $\eta' K_s$ and $K^+K^-K_s$ due to the CKM disfavored penguin contribution. As statistics improve so will the precision of the branching fractions used to calculate the limits.

All in all, the expected increase in luminosity of the two B factories promises a continuing, rich harvest of physics.

10. Acknowledgments

I should like to thank Harry Cheung and Tracey Pratt for their help and patience at every stage in the preparation of this paper. My thanks are due to

Jim Alexander, Paoti Chang and Jim Smith, authors of the Heavy Flavor Averaging Group, for enabling me to keep abreast of the rapid evolution in physics results before, during and after the Lepton Photon 2003 Symposium, and for making the task of referencing a finite one; any shortcomings are mine alone. My special thanks are due to Jim Smith, who was always at the end of a telephone or computer to help.

References

1. M. Beneke, G. Buchalla, M. Neubert and C. Sachrajda, *Nucl. Phys. B* **606**, 245 (2001).
2. M. Beneke and M. Neubert, *hep-ph/0308039*.
3. C. Chiang and J. Rosner, *Phys. Rev. D* **65**, 074035 (2002).
4. C. Chiang, M. Gronau and J. Rosner, *hep-ph/0306021*.
5. C. Chiang, M. Gronau, Z. Luo, J. Rosner and D. Suprun, *hep-ph/0307395*.
6. Y. Grossman and H. Quinn, *PRD* **58**, 017504 (1988).
7. Y. Grossman, Z. Ligeti, Y. Nir and H. Quinn, *hep-ph/0303171*.
8. BaBar Collaboration: Result contributed to Lepton Photon Symposium 2003.
9. J. Alexander, P. Chang and J. Smith, *Heavy Flavor Averaging Group*, September 2003.
10. H. Huang *et al.*, Belle Collaboration, *Phys. Rev. Lett.* **90**, 121802 (2003).
11. B. Aubert *et al.*, (BaBar Collaboration), *Phys. Rev. Lett.* **89**, 281802 (2001); M. Bona for the BaBar Collaboration, talk at FPCP (2003); B. Aubert *et al.*, (BaBar Collaboration), *hep-ex/0308012* (submitted to *Phys. Rev. Lett.* (2003)); B. Aubert *et al.*, (BaBar Collaboration), *Phys. Rev. Lett.* **91**, 021801 (2003); T. Tomura *et al.*, (Belle Collaboration), *hep-ex/0305036* (2003).
12. Belle Collaboration, presented at Lepton Photon Symposium 2003.
13. B. Aubert *et al.*, (BaBar Collaboration), *hep-ex/0308012* (submitted to *Phys. Rev. Lett.* (2003)).
14. The Particle Data Group, K. Hagiwara *et al.*, *Phys. Rev. D* **66**, 010001 (2002).
15. Y. Y. Keum and A. I. Sanda, *hep-ph/0306004* (2003).
16. M. Gronau, Private communication.
17. M. Gronau and J. Rosner, *hep-ph/0307095* (2003).
18. T. Tomura *et al.*, (Belle Collaboration), *hep-ex/0305036* (2003).
19. B. Aubert *et al.*, (BaBar Collaboration), *Phys. Rev. Lett.* **89**, 281802 (2001).
20. CDF Collaboration, presented at Lepton Photon Symposium 2003.
21. B. Aubert *et al.*, (BaBar Collaboration), *Phys. Rev. Lett.* **87**, 221802 (2001); B. Aubert *et al.*, (BaBar Collaboration), *hep-ex/0306030* (submitted to *Phys.*

- Rev. Lett.*(2003)); B. Aubert *et al.*, (BaBar Collaboration), *hep-ex/0307087* (2003); B. Aubert *et al.*, (BaBar Collaboration), *hep-ex/0308065* (submitted to *Phys. Rev. Lett.*(2003)); B. Aubert *et al.*, (BaBar Collaboration), *hep-ex/0303040* (2003).
22. H. C. Huang *et al.*, (Belle Collaboration), *hep-ex/0205062* (2002); K. Abe *et al.*, (Belle Collaboration), *BELLE-CONF-0312* EPS (2003); K. Abe *et al.*, (Belle Collaboration), *BELLE-CONF-0318* EPS (2003); A. Gordon *et al.*, (Belle Collaboration), *Phys. Lett. B* **542**, 183 (2002); K. Abe *et al.*, (Belle Collaboration), *BELLE-CONF-0317* EPS (2003); K. Abe *et al.*, (Belle Collaboration), *BELLE-CONF-0318* EPS (2003).
 23. B. Aubert *et al.*, (BaBar Collaboration), *Phys. Rev. Lett.* **91**, 051801 (2003).
 24. K. Abe *et al.*, (Belle Collaboration), *BELLE-CONF-0338* Lepton Photon Symposium 2003.
 25. M. Suzuki, *Phys. Rev. D* **66**, 054018 (2002).
 26. B. Aubert *et al.*, (BaBar Collaboration), *hep-ex/0307026* (to be published in *Phys. Rev. Lett.* (2003)); B. Aubert *et al.*, (BaBar Collaboration), *hep-ex/0308024* (2003).
 27. J. Zhang *et al.*, (Belle Collaboration), *hep-ex/0306007*2003.
 28. B. Aubert *et al.*, (BaBar Collaboration), *hep-ex/0307026* (to be published in *Phys. Rev. Lett.* (2003)); B. Aubert *et al.*, (BaBar Collaboration), *hep-ex/0309025* (submitted to *Phys. Rev. Lett.* (2003)).
 29. K. F. Chen *et al.*, (Belle Collaboration), *hep-ex/0307014* (submitted to *Phys. Rev. Lett.*(2003)); K. Abe *et al.*, (Belle Collaboration), *BELLE-CONF-0338* Lepton Photon Symposium 2003.
 30. CDF Collaboration: presented at Lepton Photon Symposium 2003.
 31. T. Browder *et al.*, (Belle Collaboration), *BELLE-CONF-0344* Lepton Photon 2003.
 32. B. Aubert *et al.*, (BaBar Collaboration), *hep-ex/0309025* (submitted to *Phys. Rev. Lett.* (2003)).
 33. B. Aubert *et al.*, (BaBar Collaboration), *hep-ex/0303046* (to be published in *Phys. Rev. Lett.* (2003)); B. Aubert *et al.*, (BaBar Collaboration), *hep-ex/0308015*2003; B. Aubert *et al.*, (BaBar Collaboration), *hep-ex/0303039* (2003).
 34. H. Aihara (for the Belle Collaboration), talk at FPCP 2003.
 35. H. Lipkin, *Phys. Lett. B* **254**, 247 (1991).
 36. R. Aleksan *et al.*, *hep-ph/0301165* (2003).

DISCUSSION

Gerhard Buchalla (LMU Munich): Concerning the high experimental value of $B(B^0 \rightarrow \pi^0\pi^0)$ compared to the theoretical calculations, the prediction is much more uncertain than that of most other decay modes. The reason is that this decay is “color-suppressed” and thus accidentally small and extremely uncertain at LO. It is thus very sensitive to NLO effects and susceptible to other corrections. Very important further information on this issue could also come from comparing the decay $B^+ \rightarrow \pi^+\pi^0$ with the semileptonic decay $B \rightarrow \pi l\nu$.

John Fry: I accept what you say. However, this should make $B^0 \rightarrow \pi^0\pi^0$ an interesting theoretical test bed for NLO effects, in the same way that measurements of A_{CP} are sensitive to them.

George W. S. Hou (National Taiwan University): There is an indication for rescattering, despite the small BF for $B \rightarrow K^+K^-$. In $\pi\pi \rightarrow \pi\pi$, $K\bar{K}$ rescattering, there are actually two rescattering phases. In a paper with C.K. Chua and K.C. Yang, we find 30% of the parameter space where K^+K^- can be suppressed, while a large $\pi^0\pi^0$ and opposite sign A_{CP} for $K^-\pi^+$ mode can be accounted for. The interest is in fact in CP-asymmetries in the $\pi^+\pi^-$ mode, which can be

large.

John Fry: It would be interesting to see quantitative predictions which account for all the data, including the small BF for $B^+ \rightarrow \psi\pi^+$.

Jonathan Rosner (University of Chicago): The nearly complete longitudinal polarization in $B \rightarrow \rho\rho$ decays is not a surprise since factorization seems to work well in processes dominated by a color-favored tree amplitude. Similarly in $B \rightarrow \phi K^*$ the presence of a substantial p-wave component, leading to R (perpendicular) not equal to zero, indicates that the parity conserving component of the $b \rightarrow s$ penguin amplitude is more significant than anticipated in factorization, as also seems true in $B \rightarrow VP$ decays. The puzzle is $B^+ \rightarrow \rho^0 K^{*+}$, which appears to be almost completely longitudinal – though presumably dominated by the same penguin amplitude(s) as $B \rightarrow \phi K^*$. It seems hard to describe both $B^+ \rightarrow \rho^0 K^{*+}$ and $B \rightarrow \phi K^*$ polarizations simultaneously within the Standard Model.

John Fry: Further theoretical guidance will be welcomed, especially if the measurement of additional final states can help to resolve the situation.